Accepted Manuscript online: 2023-10-31 Article published online: 2024-02-16

Original Article

Exosomal CircMFN2 Enhances the Progression of Pituitary Adenoma via the MiR-146a-3p/TRAF6/NF-κB Pathway

Haitong Wan[1] Xiang Gao[1] Zexu Yang[2] Leiguo Wei[2] Yufei Qu[2] Qi Liu[2]

[1] Department of Neurosurgery, First Affiliated Hospital of Medical College, Shihezi University, Shihezi, China
[2] Department of Neurosurgery, First Affiliated Hospital of Medical College, Shihezi University, Shihezi, China

Address for correspondence Qi Liu, PhD, Department of Neurosurgery, First Affiliated Hospital of Medical College, Shihezi University, Shihezi, China (e-mail: liuqi801020@163.com).

J Neurol Surg A Cent Eur Neurosurg

Abstract

Background Pituitary adenoma (PA) is a common intracranial endocrine tumor, but no precise target has been found for effective prediction and treatment of PA.

Methods Quantitative reverse transcription polymerase chain reaction (qRT–PCR) analysis showed that circMFN2 could affect the expression of miR-146a-3p in PA samples. Moreover, we used Western blotting to evaluate the expression levels of TRAF6 and NF-κB markers. The EdU assay, scratch wound healing assay, and Matrigel invasion assay were performed to assess the potential function of this pathway in PA cells. Based on the bioinformatic analysis including KEGG, gene ontology (GO) analysis, and microarray analysis, we evaluated the efficacy of circMFN2 as a potential biomarker for diagnosing PA, and we aimed to determine the mechanism of action in PA cells.

Results Our findings indicate that there is a significant increase in the expression of circMFN2 in tissues, serum, and exosomes in the invasive group compared with the noninvasive and normal groups. Furthermore, this difference was statistically significant both preoperatively and postoperatively. To clarify its function, we downregulated this gene, and the experimental results suggested that the motility and proliferative capacity were reduced in vitro. In addition, rescue assays showed that miR-146a-3p could successfully reverse the inhibitory effect of circMFN2 knockdown on motility and proliferation in PA cells. Moreover, downregulation of circMFN2 and miR-146a-3p significantly changed the expression of TRAF6 and NF-κB.

Conclusion This study identified that circMFN2 regulates miR-146a-3p to promote adenoma development partially via the TRAF6/NF-κB pathway and may be a potential therapeutic target for PA.

Keywords
- pituitary adenoma
- circMFN2
- miRNA
- exosome
- biomarker

received
August 6, 2023
accepted after revision
October 24, 2023
accepted manuscript online
October 31, 2023

DOI https://doi.org/10.1055/a-2201-8370.
ISSN 2193-6315.

© 2024. The Author(s).
This is an open access article published by Thieme under the terms of the Creative Commons Attribution-NonDerivative-NonCommercial-License, permitting copying and reproduction so long as the original work is given appropriate credit. Contents may not be used for commercial purposes, or adapted, remixed, transformed or built upon. (https://creativecommons.org/licenses/by-nc-nd/4.0/)

Georg Thieme Verlag KG, Rüdigerstraße 14, 70469 Stuttgart, Germany

Introduction

Pituitary adenoma (PA) is a common neuroendocrine tumor originating from pituitary cells in the sella turcica and is second only to glioma and meningioma (MA) in terms of incidence. Almost 25 to 55% of PAs show invasive growth,[1] manifested by local infiltration that causes the destruction of adjacent tissues, such as the cavernous sinus, sella turcica, and hypothalamus; these tumors are called invasive PAs.[2] Invasive PAs are challenging to diagnose, and almost 50% of patients have varying degrees of residual tumor after surgery, which may lead to recurrence and a poor prognosis. Molecular markers that can accurately predict the prognosis of PA patients have been unsatisfactory.[3] Consequently, it is necessary to study the detailed mechanism underlying invasive PA development in depth, identify target genes for the treatment of invasive PA, and provide a new experimental basis for the targeted therapy of PA.

Circular ribonucleic acids (circRNAs) are noncoding RNAs. The presence of a large number of circRNAs greatly increases the complexity of the human transcriptome. These molecules form a heterogeneous class of RNAs that lack protein coding function. CircRNAs play key roles in the regulation of transcriptional and posttranscriptional processes, including X chromosome inactivation, epigenetic regulation, genomic imprinting, and mRNA splicing.[4] In 2010, with the advent of high-throughput sequencing and bioinformatics analysis of the nonpolyadenylated transcriptome, thousands of circRNAs were discovered and found to be diverse and genetically and structurally stable throughout the genome.[5–8] There is growing evidence that circRNAs are associated with the occurrence of different diseases.[9] Most circRNAs exert regulatory functions by competitively binding with microRNAs (miRNAs). Studies have reported that circ_0001368 can promote the proliferative ability of gastric cancer cells through the miRNA-6506–5p/FOXO3 pathway.[10]

This study investigates the role of circMFN2, a newly identified circRNA in the high-throughput microarray of PA, in the diagnosis and mechanism of action of PA. The study evaluates circMFN2 expression in serum, exosomes, and tumor tissues of PA patients and found it to be a potential molecular marker for the diagnosis of PA. The study also explores and verifies that circMFN2 could regulate miR-146a-3p to increase the proliferation and invasive function of PA cells, partly through the TRAF6/NF-κB pathway. This study provides valuable insights into the role of circMFN2 in the diagnosis and mechanism of action of PA. This finding also showed that circMFN2 is involved in the progression of PA and can act as a critical molecular marker for PA diagnosis.

Methods

Pituitary Adenoma Microarray Analysis

CircRNA microarray assays were performed on five pairs of nonfunctioning PAs and normal tissues and used to identify differentially expressed noncoding RNAs. All microarray data were downloaded from the GEO database (http://www.ncbi.nih.gov/geo). The raw data were downloaded as MINiML files. The raw sequencing data underwent preprocessing using FastQC and cutadapt software. The resulting clean reads were then mapped to hg38 and circBase using Tophat and MapSplice software. The limma package in the R software was used to study the differentially expressed circRNA and miRNA. Differential expression analysis of RNAs was conducted using the R package EdgeR (http://www.R-project.org) with the criteria of $|\text{Fold change}| > 2$ and p value <0.01. All statistical analyses and graphics were performed using R. ClusterProfiler package (version: 3.19.0) in R was employed to analyze the GO function of potential targets and enrich the KEGG pathway; the R software pheatmap package was used to draw heatmap. The statistical method for gene expression comparisons was the Wilcox-tests method.

Collection of Patients' PA Tissues and Serum

We enrolled 50 serum samples obtained from patients of The First Affiliated Hospital of Medical College of Shihezi (Shihezi, China). Prior to the research, none of the patients underwent surgery or therapy. Healthy human serum samples were collected from 50 volunteers without underlying diseases in the department. Fresh tissue specimens were frozen in a –80°C refrigerator for quantitative reverse transcription polymerase chain reaction (qRT–PCR) analysis. ►**Supplementary Table S2** shows the clinicopathologic parameters of the patients. We used magnetic resonance imaging (MRI) + Knosp grades to determine the invasiveness of PAs. All the patients' blood and tissue were collected with written signed consent and validated by the Ethics Committee of The First Affiliated Hospital of Medical College of Shihezi (KJ2021–076–02).

Serum Exosome Isolation

The samples were subjected to centrifugation at 3,000 × g for 30 minutes to separate serum and blood cells. The resulting supernatant was then subjected to further centrifugation at 10,000 × g for 30 minutes, followed by an additional round of centrifugation at 10,000 × g for 70 minutes at 4°C. The aqueous layer was filtered using a 0.22-μm filter to separate it from the solid layer, and the resulting exosome pellet was resuspended in phosphate-buffered saline (PBS).

TEM

The exosome suspension was diluted in 0.5 mg/mL with PBS, and then spotted onto a glow-discharged copper grid placed on a filter paper and dried for 10 minutes by exposure to infrared light. Next, the exosome samples were stained with one drop of phosphotungstic acid (1% aqueous solution) for 5 minutes and dried for 20 minutes by exposure to infrared light. Finally, the exosomes were visualized under a transmission electron microscope (Thermo Fisher Scientific, Waltham, Massachusetts, United States) at 100 keV.

Nanoparticle Tracking Analysis

The collected exosomes were suspended in a PBS solution and thoroughly mixed. A portion of the exosomes was filtered through a Millipore filter, while the remaining solution was diluted to ensure that the exosomes were clearly

visible in the solution alone. The exosomes were then assayed using NanoSight N300 (Worcestershire, UK).

Cell Culture and Transfection

The PA cell lines, including GH3 and MMQ, were sourced from Procell (Wuhan, China). The cells were placed in the incubator at 37°C with 5% CO_2 and seeded on a special medium for GH3 cells, including a mixture of Ham's F-12K, 15% horse serum (HS), 2.5% fetal bovine serum (FBS), and 1% penicillin–streptomycin (P/S). The medium was changed every 2 to 3 days, and 1 mL of special medium was added during each change. Experiments were conducted until the cells reached 80% density. The cell growth cycle was approximately 5 to 7 days. PA cells were transfected with siRNA using Lipofectamine 3000, encompassing RNAi and NC (GenePharma, Shanghai, China). In our study, we utilized a six-well plate for transfection procedures. Specifically, we added 8 µL of Lipofectamine 3000 and 4 µL of RNAi to each well. Then, the cells were incubated for 24 to 48 hours until the constructed plasmid was in the cells and siRNA was downregulated in the cells. qRT–PCR was used to validate the transfection efficiency of siRNA. The successful transfection was determined based on achieving a change of approximately 60 to 80% in the expression of the experimental group compared with the NC group.

Cell Proliferation Assay

According to the instructions provided by the APExBIO EdU In Vitro Imaging Kit, the EdU assay was performed (APExBIO, Houston, Texas, United States). Briefly, 20-M EdU was incubated with the treated cells in six-well plates for one night. Afterward, the cells were fixed with 4% paraformaldehyde and washed with PBS. After that, each well received 1 mL of PBS blended with 5 µL of Triton X-100, which was incubated in a cell incubator for 20 minutes. Then, a click reaction solution was configured for click reaction. Each well was washed with 1 mL PBS to remove the washing solution before being stained with 1 mL 1 × Hoechst 33342 and incubated for 30 minutes. Using a fluorescence microscope, pictures were taken (Olympus, Tokyo, Japan). The proliferation rate was determined as the proportion of EdU-positive cells. In 96-well plates, we cultured the transfected cells and incubated them for 24 hours. Then, 10 µL of CCK-8 reagent was added to each well in a 96-well plate and incubated for 4 hours. At 450 nm, we collected experimental data using THERMO Multiskan GO (THERMO, Suzhou, China) each 2 hours.

Matrigel Invasion Assay

The Transwell chamber system (Costar, Corning, New York, United States) was used to perform the Matrigel invasion assay. The system is equipped with a polycarbonic membrane. Single PA cells were suspended in a serum-free medium at a density of 10^5 cells/mL. Then, we added PA cells into the upper compartment containing 200 µL of serum-free medium with Matrigel. We pipetted 600 µL of culture medium for pituitary tumor cells consisting of 15% HS into the bottom 24-well plate. After standing in the incubator for 48 hours, the cells penetrated the membrane and grew on the lower surface of the chamber with Matrigel. The top surface of the membrane was cleaned with cotton swabs to remove any nonmigrating cells. After 4% paraformaldehyde fixation and crystal violet staining, stained cells were photographed using an Olympus fluorescence microscope. Three photographs of each area of invasive cells were taken, and the number of stained cells was calculated independently.

Wound Healing Assay

PA cells were transfected and cultured in six-well plates until their numbers reached 1×10^6. They were starved for 24 hours using Dulbecco's modified eagle medium (DMEM). A 200-µL pipette tip was used to create a wound (time 0), the detached cells were washed off, and then serum-free DMEM was used for culture. After 48 hours, photographs of five nonoverlapping fields were taken.

Total RNA Isolation and qRT–PCR Analysis

A plasmid Midi Kit (QIAGEN, Hilden, Germany) was used to isolate serum total RNA. RNA extraction, including tissues and cells, was performed using the TRIzol method according to the reagent manufacturer's instructions. Nanodrop (Thermo Fisher Scientific) was used to check the RNA purity and concentration just like OD260/OD280 in the range of 1.8 to 2.1 and RNA concentration more than 900 ng/µL. For reverse transcription, the purified RNA was subjected to the TIANScript II RT kit (TIANGEN, Beijing, China). Next, FastReal qPCR PreMix (SYBR Green) was used to conduct qRT–PCR experiments. qRT–PCR experiments were performed using the 7,500 fast system. Please refer to the supplementary materials for specific reaction conditions. We used U6 and β-actin as reference genes for PCR experiments (►**Supplementary Table S1**, available in the online version only). Each experiment was performed in triplicate.

Western Blot

To extract the protein, 1 mL of RIPA buffer was added to the cells and we waited for 15 minutes. This process was done on ice. The protein solution (∼15 mL) was subjected to 10% sodium dodecyl sulfate (SDS) polyacrylamide gel electrophoresis. Power was turned on and the voltage level was initially set to 100 V. After 20 minutes, the voltage was adjusted to 220 V and electrophoresis was continued for 60 minutes. Subsequently, the proteins were transferred to a polyvinylidene difluoride (PVDF) membrane. Next, pretreat the PVDF membrane in anhydrous ethanol for 2 hours. The electrotransfer switch was turned on and the current maintained at 300 mA for 90 minutes. Once the electrorevolution was complete, power was turned off. The PVDF membrane was submerged in the containment solution for 1 hour. The primary antibody and the PVDF membrane were placed together in the antibody tube and incubated overnight on a low-temperature shaker. The PVDF membrane was placed in sealing liquid for 1 hour. The PVDF membrane in the overnight antibody tube was put into the tank of TBST,

 © 2024. The Author(s).

washed for 5 minutes, added into the antibody tube of the second antibody, and incubated for 1 hour. The membrane strip was placed in the water channel again and washed for 5 minutes. The color solution was added to the dish where the film strip was placed, and the darkroom exposure system was used for imaging and analysis. Glyceraldehyde-3-phosphate dehydrogenase (GAPDH) served as a loading control.

Target Prediction

The TargetScan and CircBase databases can be used to predict the potential targets of circMFN2. This prediction was performed for miRNA targets in human tissues and rat cells. For subsequent validation experiments, the top three were combined.

Statistical Analysis

GraphPad Prism software (GraphPad Software, San Diego, California, United States) was used for all experimental data analyses. Correlation analysis of genes and statistical analysis of clinical data between different groups were performed using the *t*-test. The diagnostic efficacy evaluation of circMFN2 was analyzed by receiver operating characteristic (ROC) curves. A p value of less than 0.05 was considered statistically significant. Spearman's analysis was performed for analysis of correlation between circMFN2, miR-146a, TRAF6, and NF-κB. The difference between the two sides was statistically significant ($p < 0.05$).

Results

Identification of Differentially Expressed circRNAs in PA

We conducted high-throughput circRNA microarray assays on five pairs of pituitary samples from patients with PA and normal subjects. We utilized a volcano plot and heatmap to display genes with significant expression differences. We found 6,656 upregulated genes and 2,156 downregulated ncRNA genes by testing (►**Fig. 1A**), and ►**Fig. 1B** shows the heatmap of these differentially expressed genes. We screened the signaling pathway RNAs related to adenoma growth and invasion by doing KEGG pathway and GO analysis[11–15] on the above high-throughput microarray (►**Fig. 1C**). In our study, we compared the top 50 expressed circRNAs and found that circMFN2 satisfied the aforementioned conditions ($p < 0.05$, adjusted $p < 0.05$, fold change = 2). To validate its role in other chips, we selected GSE51618 and grouped individuals as invasive, noninvasive, and normal. After conducting the assay, we observed a statistically significant difference in the expression of circMFN2 in the pituitary gland of the invasive and noninvasive groups (G1 group) compared with normal individuals (G2 group), as shown in ►**Fig. 1D**.

circMFN2 Expression in PA Patients and ROC Curve Analysis

We confirmed the presence of circMFN2, which is located on chromosome 1. This circRNA is derived from an exonic region

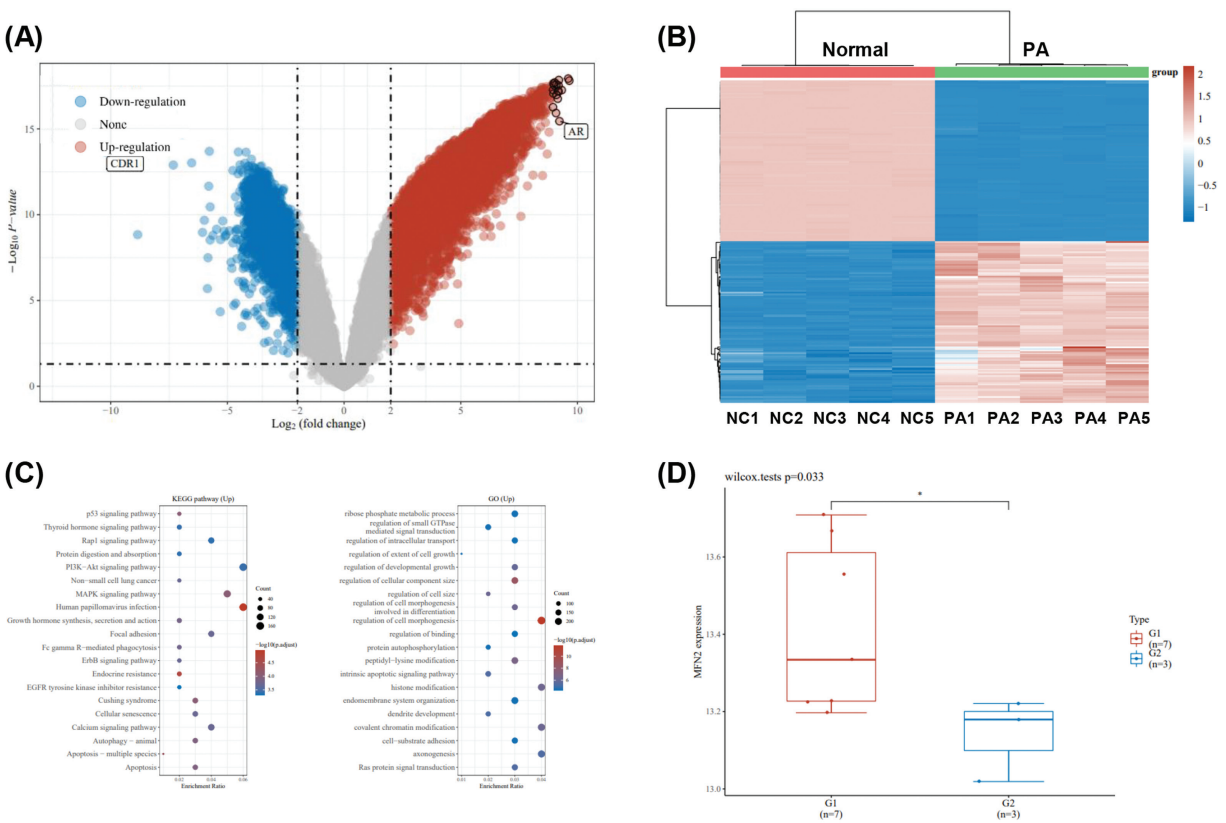

Fig. 1 Expression profiles of lncRNAs in PA.

 © 2024. The Author(s).

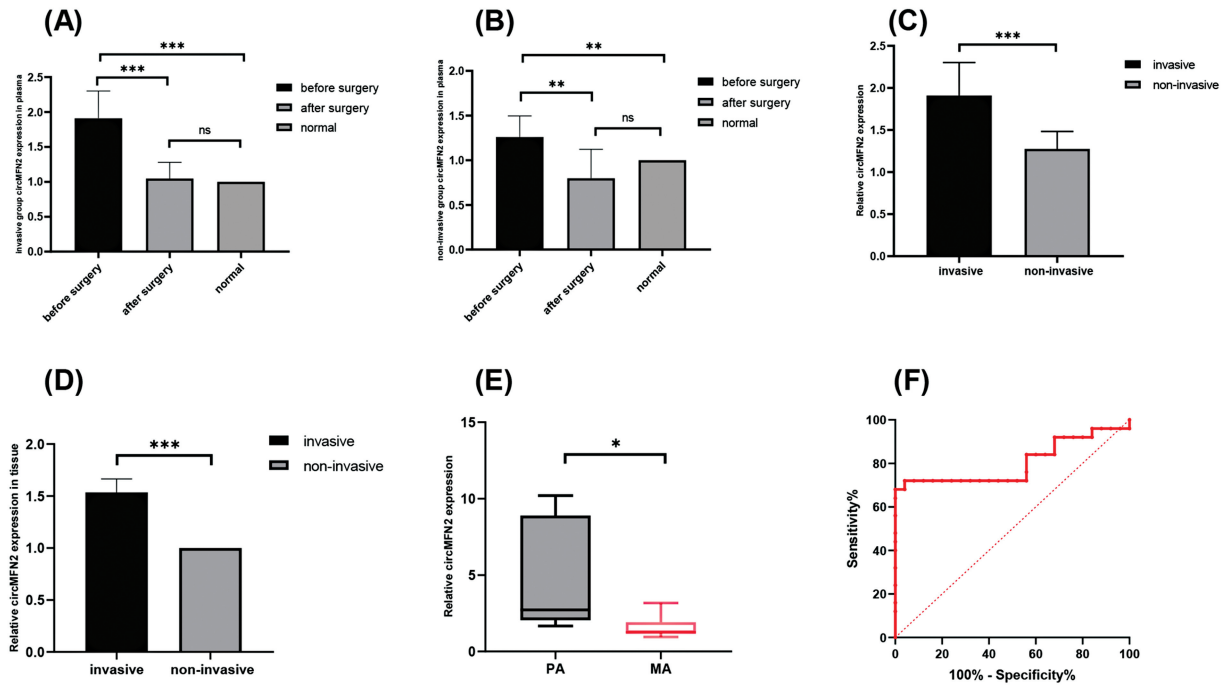

Fig. 2 Relative circMFN2 expression in serum and tissues and its diagnostic efficiency.

of the MFN2 gene and has a length of 315 nucleotides. The confirmation was done using circbank (http://www.circbank.cn). To investigate the correlation between the expression of circMFN2 and PA pathogenesis, we selected 28 cases from a sample of 50 serum samples collected for the experiment. We collected the tissue specimens of eight PA and MA patients to investigate the difference in expression of circMFN2 in PAs and MAs. First, we divided the patients into invasive and noninvasive groups. In the invasive group, serum circMFN2 expression was significantly upregulated before surgery compared with that after surgery and overall exhibited higher expression levels compared with those in the healthy control group (►**Supplementary Table S1**, available in the online version only and ►**Fig. 2A**). Compared with the noninvasive group, the invasive group exhibited significantly upregulated serum circMFN2 expression before surgery, and there was no significant differential expression between the healthy controls and either of the groups after surgery (►**Fig. 2B**). Moreover, circMFN2 expression was not significantly different between the invasive and noninvasive groups after surgery. In both tissues and serum, we found that the expression levels of circMFN2 was significantly higher in the invasive group than in the noninvasive group (►**Fig. 2C, D**). Statistical analysis of the patient data showed that the expression of circMFN2 was closely related to the invasiveness of PA (►**Supplementary Tables S2** and **S3**, available in the online version only). Second, extensive deposition of circMFN2 was observed in PA tissues compared with that in other brain tumor tissues, such as MA. The Mantel–Cox test revealed that the expression of circMFN2 in MA tissues was downregulated compared with that in PA tissues (►**Fig. 2E**). The purpose of this part was to investigate the differential expression of circMFN2 in PA compared with other common intracranial tumors. Finally, we used circMFN2 as a test variable, normal and adenoma groups as the status scalars, and MRI + pathologic diagnosis as the gold standard to construct the ROC curve. The ROC curve area of circMFN2 was 0.802 (►**Fig. 2F**), and the model could distinguish healthy individuals from PA patients.

Exosomal circMFN2 Expression in PA Patients

We utilized ultracentrifugation to isolate exosomes from the serum of patients with PA. Our results, which were obtained through the use of WB, NTA, and TEM, indicated the presence of exosomes with a mean particle size of approximately 150 nm and positive surface markers (►**Fig. 3A–C**). Then we used qRT–PCR to detect the expression of circFMN2 in serum exosomes of 50 patients with PA and 50 normal people (►**Supplementary Table S4**, available in the online version only). The study found that the expression of circFMN2 in serum exosomes was significantly higher in patients with invasive PA before surgery compared with those with noninvasive PA and normal individuals. Similarly, the expression of circFMN2 was also elevated in serum exosomes of patients with noninvasive PA before surgery as compared with normal individuals (►**Fig. 3D**). The content of circFMN2 in serum exosomes of patients with PA after surgery was higher than that in serum exosomes of normal people. Compared with the normal group, circFMN2 was higher in serum exosomes of patients with invasive PA after surgery. There was no significant difference in the expression of circFMN2 in serum exosomes between the noninvasive PA group and normal human serum exosomes after surgery (►**Fig. 3E**). The data presented are consistent with the findings of circMFN2 in the sera of patients with PA,

 © 2024. The Author(s).

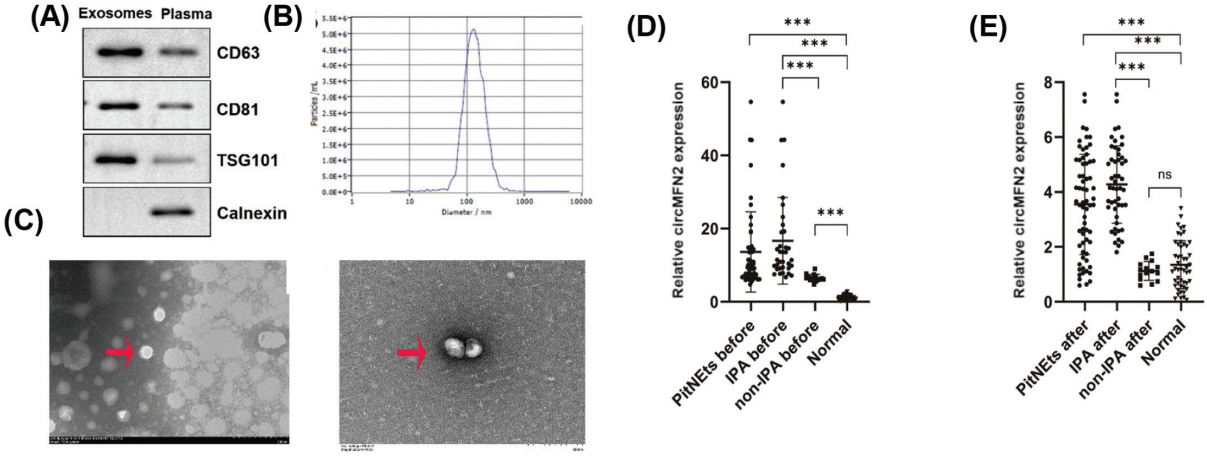

Fig. 3 Relative circMFN2 expression in exosome.

suggesting that circMFN2 has potential as a molecular marker for diagnosing PA in both serum and exosomes.

CircMFN2 Promotes Motility and Tumorigenesis in PA Cells

To investigate the mechanism of action of circMFN2 in PA cell proliferation and development, we transfected siRNA to downregulate the expression of circMFN2 in GH3 and MMQ cells. The transfection results were determined using qRT–PCR (►**Fig. 4A**). After siRNA transfection, EdU staining and CCK-8 assays were used to evaluate whether cell proliferation was decreased. As shown in ►**Fig. 4B, C**, the proliferation rate of the si-circMFN2 group was significantly lower than that of the si-NC group. Transfection with the siRNA effectively inhibited the growth of PA cells. Wound healing and Matrigel invasion assays were conducted to evaluate migration and invasion. There was a significant difference between the si-circMFN2 and si-NC groups. The mobility of the si-circMFN2 group was markedly less than that of the si-NC group. Downregulated circMFN2 lowered cell motility (►**Fig. 4D, E**). Overall, the results demonstrated that circMFN2 knockdown could limit the proliferation, migration, and invasion of PA cells.

CircMFN2 and miR-146a-3p May Act as Molecular Sponges That Promote the Invasiveness of PA Cells

We performed further analyses to validate that circMFN2 regulates PA cells. We identified the predicted targets of circRNA and miRNA through the TargetScan software. We screened the downstream genes and selected three miRNAs with high correlation. The three genes included miR-3084a-5p, miR-509–5p, and miR-146a-3p (►**Fig. 5A**). To validate the predictions, we performed qRT–PCR in GH3 and MMQ cells. ►**Fig. 5B and C** shows the expression of each gene in PA cells, and we selected miR-146a-3p, which was most differentially expressed in the two cell lines, as the experimental gene. To further validate this finding, we co-transfected GH3 and MMQ cells with miR-146a-3p mimic and inhibitor and observed circMFN2 expression. The results indicated that the miR-146a-3p mimic downregulated the expression of circMFN2 compared with that in the NC group, and the miR-146a-3p inhibitor upregulated circMFN2 expression in GH3 and MMQ cells (►**Fig. 5D, E**). We also analyzed five nonfunctional PA specimens and five normal human pituitary specimens using bioinformatic tools. The findings revealed a statistically significant decrease in miR-146a expression in nonfunctional PA specimens compared with normal human pituitary specimens (►**Fig. 5F**). Although miR-3084a-5p and miR-509–5p were not detected, the high-throughput microarray results matched the cellular results, indicating that miR-146a-3p may regulate the expression of circMFN2 in PA cells. Additionally, these two genes are negatively correlated and may function as molecular sponges to promote the progression of PA.

MiR-146a-3p Inhibits Motility and Proliferation via circMFN2 in PA Cells

We conducted several explorations to investigate the mechanism of miR-146a-3p's action as a circMFN2 sponge and its impact on PA cells in PA cell lines. We cultured the PA cell lines with upregulated and downregulated miR-146a-3p. We also conducted rescue experiments by simultaneously downregulating circMFN2 and miR-146a-3p in PA cells to determine if the inhibitory effect of si-circMFN2 on cells could be reversed. The results showed that PA cell proliferation and migration were inhibited through the miR-146a-3p mimic. The miR-146a-3p inhibitor promoted motility and tumor growth (►**Fig. 6**). The experimental results also showed that the proliferation, migration, and invasion abilities of the group co-transfected with miR-146a-3p inhibitor and si-circMFN2 were enhanced to different degrees compared with those in the group transfected with si-circMFN2 or miR-146a-3p mimic alone. This finding suggested that si-circMFN2 could be partially rescued by the miR-146a-3p inhibitor to attenuate the inhibition of proliferation, invasion, and migration of PA cells. Thus, we experimentally observed that miR-146a-3p, as a suppressor gene in PA cells, could regulate the oncologic function of PA by downregulating the expression of circMFN2.

 © 2024. The Author(s).

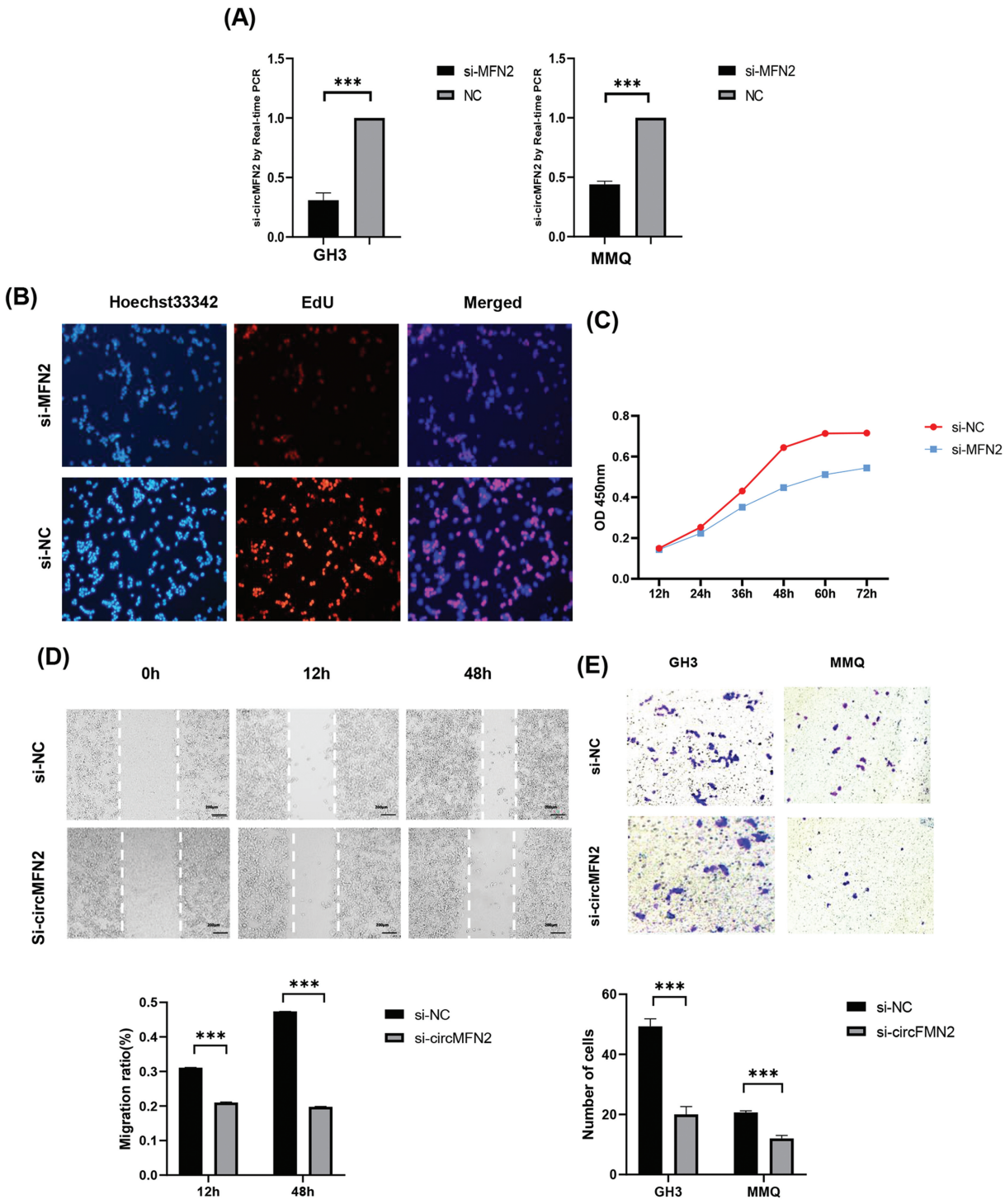

Fig. 4 CircMFN2 promotes proliferation, migration and invasion in PA cells.

circMFN2 Affected PA Tumorigenesis by Binding to miR-146a-3p to Regulate the TRAF6/NF-κB Signaling Axis

To further explore the signaling pathway through which circMFN2 regulates the PA pathogenesis, after analyzing high-throughput RNA microarrays from 5 pairs of normal subjects and patients without functional PA, we identified 9,000 upregulated and downregulated genes. We used TargetScan software to screen the downstream mRNA of miR-146a-3p; the algorithm excluded false-positive specimens and identified TRAF6 and NF-κB as potential downstream mRNA molecules of miR-146a-3p (►**Fig. 7A, B**). Our study utilized high-throughput microarrays to analyze the gene expression of TRAF6 and NF-κB. Our findings indicate that these genes were upregulated in nonfunctional PAs, with their expression being lower in normal human controls than in PA controls. To verify consistency between results in pituitary tumor cells and tissues, PA cells were transfected

 © 2024. The Author(s).

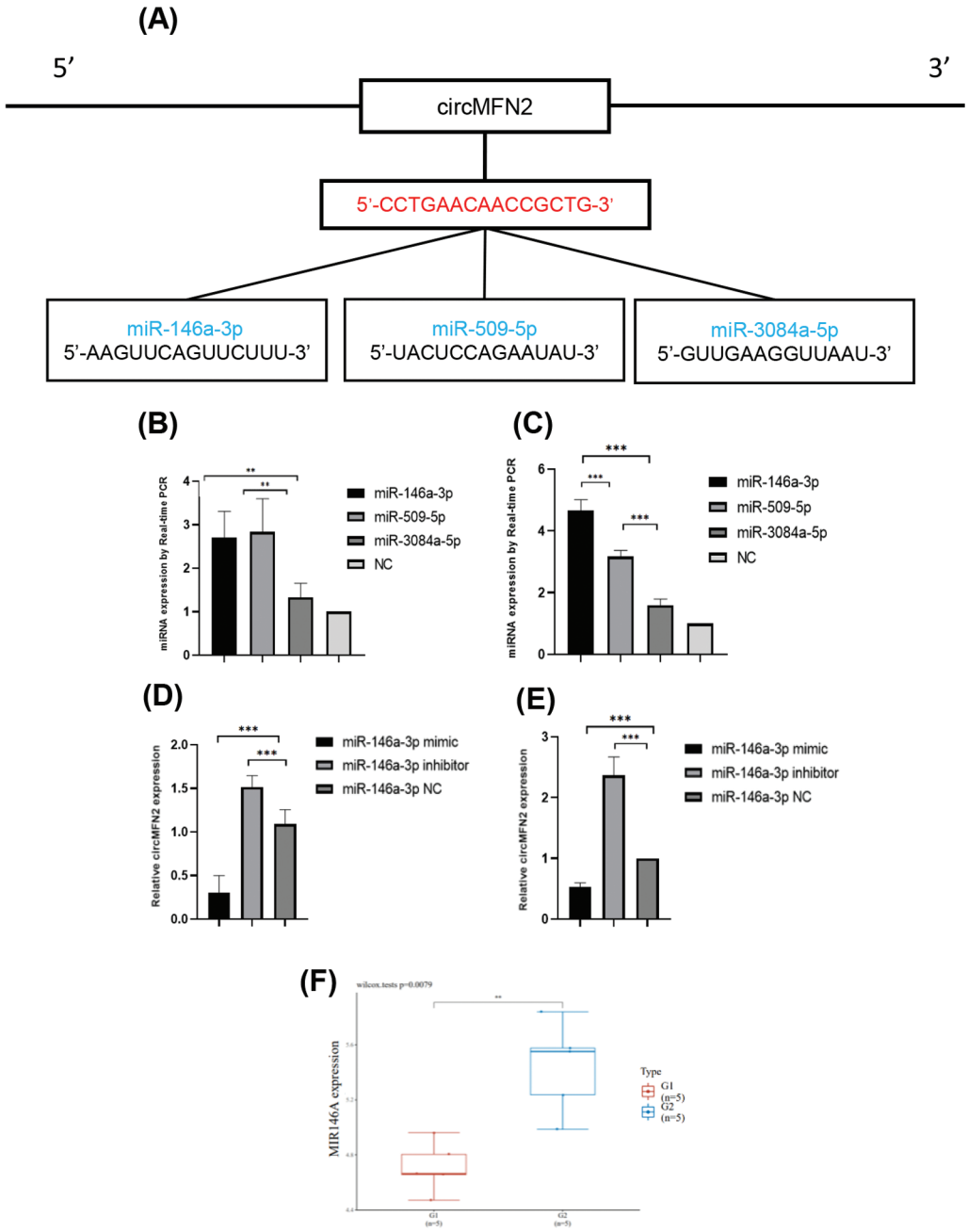

Fig. 5 CircMFN2 maybe as the miRNA sponge for miR-146a-3p.

with si-circMFN2, miR-146a-3p mimic, and miR-146a-3p inhibitors. Western blotting was then used to evaluate TRAF6 and NF-κB protein expression levels in the PA cells. The results indicated that the TRAF6 and NF-κB expression levels were significantly higher in the transfected si-circMFN2 group compared with the control group and the si-circMFN2 NC group (►**Fig. 7C, D**). Moreover, when we knocked down, the miR-146a-3p, TRAF6, and NF-κB expression levels were higher than those in the NC group. After transfection with the miR-146a-3p mimic, the TRAF6 and NF-κB expression levels were significantly downregulated compared with those in the NC group (►**Fig. 7E, F**). We concluded through a correlation analysis that the expression levels of TRAF6 and NF-κB were positively correlated (►**Fig. 7G**). circMFN2 expression was positively correlated to TRAF6 protein expression (►**Fig. 7H**). The same was true for NF-κB (►**Fig. 7I**). MiR-146a-3p expression was negatively correlated with the TRAF6 and NF-κB expression levels (►**Fig. 7J, K**). Therefore, circMFN2 may promote the proliferation, migration, and invasion of PA by sponging miR-146a-3p via the TRAF6/NF-κB signaling axis.

Discussion

PA accounts for approximately 15% of all intracranial tumors in China. It is the third most common intracranial tumor in terms of incidence. Almost 25 to 55% of cases of PA exhibit invasion and local immune cell infiltration, causing

 © 2024. The Author(s).

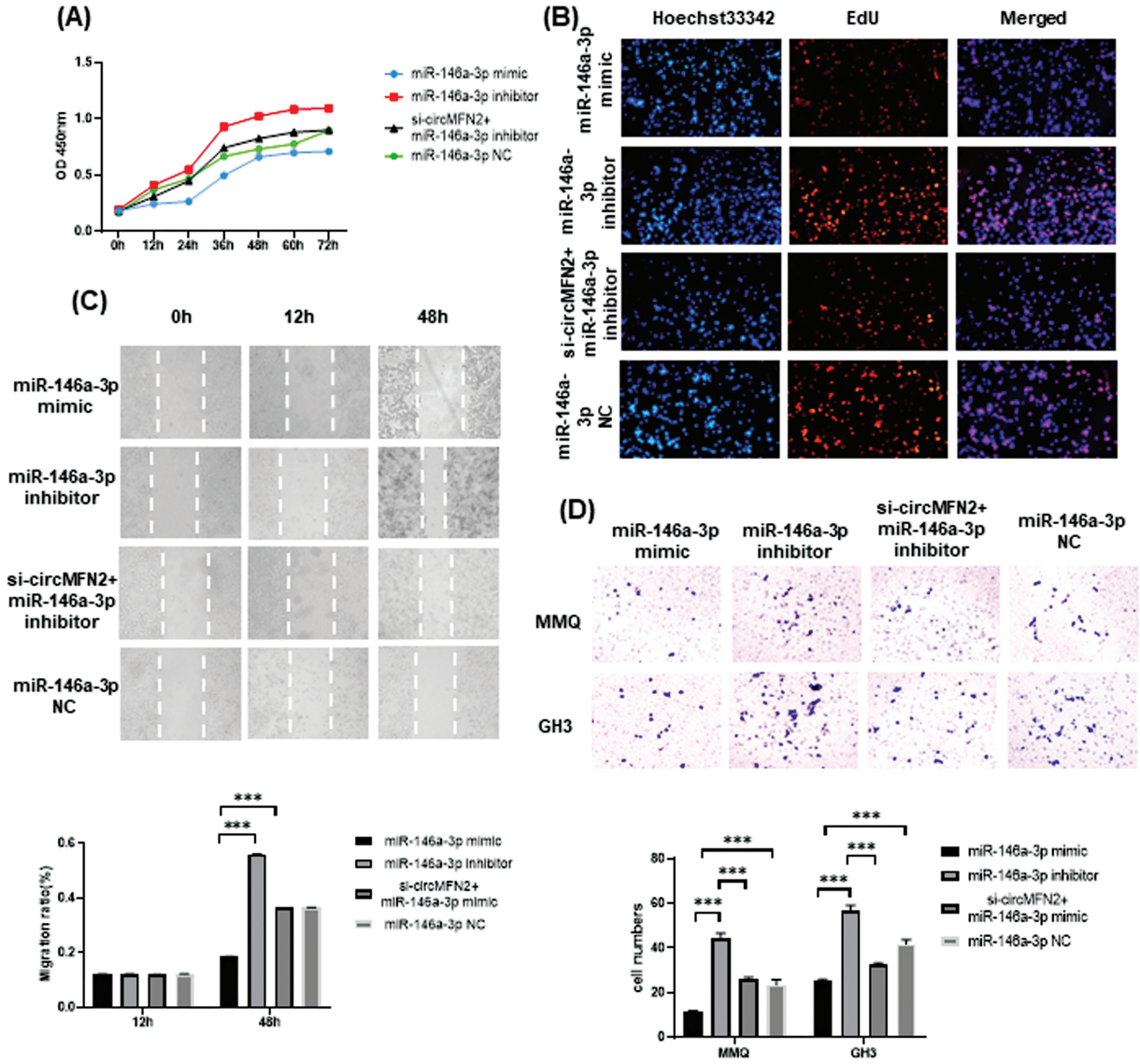

Fig. 6 miR-146a-3p promotes proliferation, migration and invasion via circMFN2 in PA cells.

destructive changes in adjacent tissues.[16] The pathogenesis of PA is a complex process that involves multiple factors and has not yet been clarified. It has been theorized that the lack of early biomarkers in many patients with PA is attributed to endocrine disease and nerve compression.[17] Furthermore, PA patients are challenging to identify in current medical diagnoses, and they often experience various adverse reactions during treatment.[18] Since the tumor arises from the pituitary gland, which resides outside of the blood–brain barrier, serum molecular markers and therapeutic targets may be able to effectively predict the prognosis of PAs.[19] CircRNAs are candidate biomarkers because of their stable structure, tissue specificity, and high expression in human tissues and body fluids.[20] The insensitivity and stability of circRNAs to ribonucleases have made circRNAs a popular research topic.[21] An increasing number of circRNAs associated with multiple diseases are being discovered and verified.[22] In general, encouraging results have been reported by exploring the functions of these circRNAs.

CircRNAs, which are noncoding RNAs with a circular structure, have the ability to regulate mRNA stability and gene transcription in cells. They can also act as miRNA sponges to control gene expression. Additionally, circRNAs are directly involved in the processes of proliferation, apoptosis, and differentiation of neuronal cells and tumor cells.[23] Hsa_circ_0004872, identified as a molecular sponge, has been found to regulate the development of gastric carcinogenesis and gastric cancer by binding to miR-224.[24] Another study revealed that circ_0009910 is associated with the growth, invasion, and migration of gastric cancer tumors, osteosarcoma, and chronic granulocytic leukemia.[25–27] Although most circRNAs are noncoding RNAs, a few of them have the ability to encode polypeptides. These circRNAs, which can encode polypeptides, not only act within their own cells but can also be secreted into the intercellular matrix through exosomes. This allows them to communicate and transmit information to other cells, leading to changes in the biological properties of the surrounding cells.[28,29]

 © 2024. The Author(s).

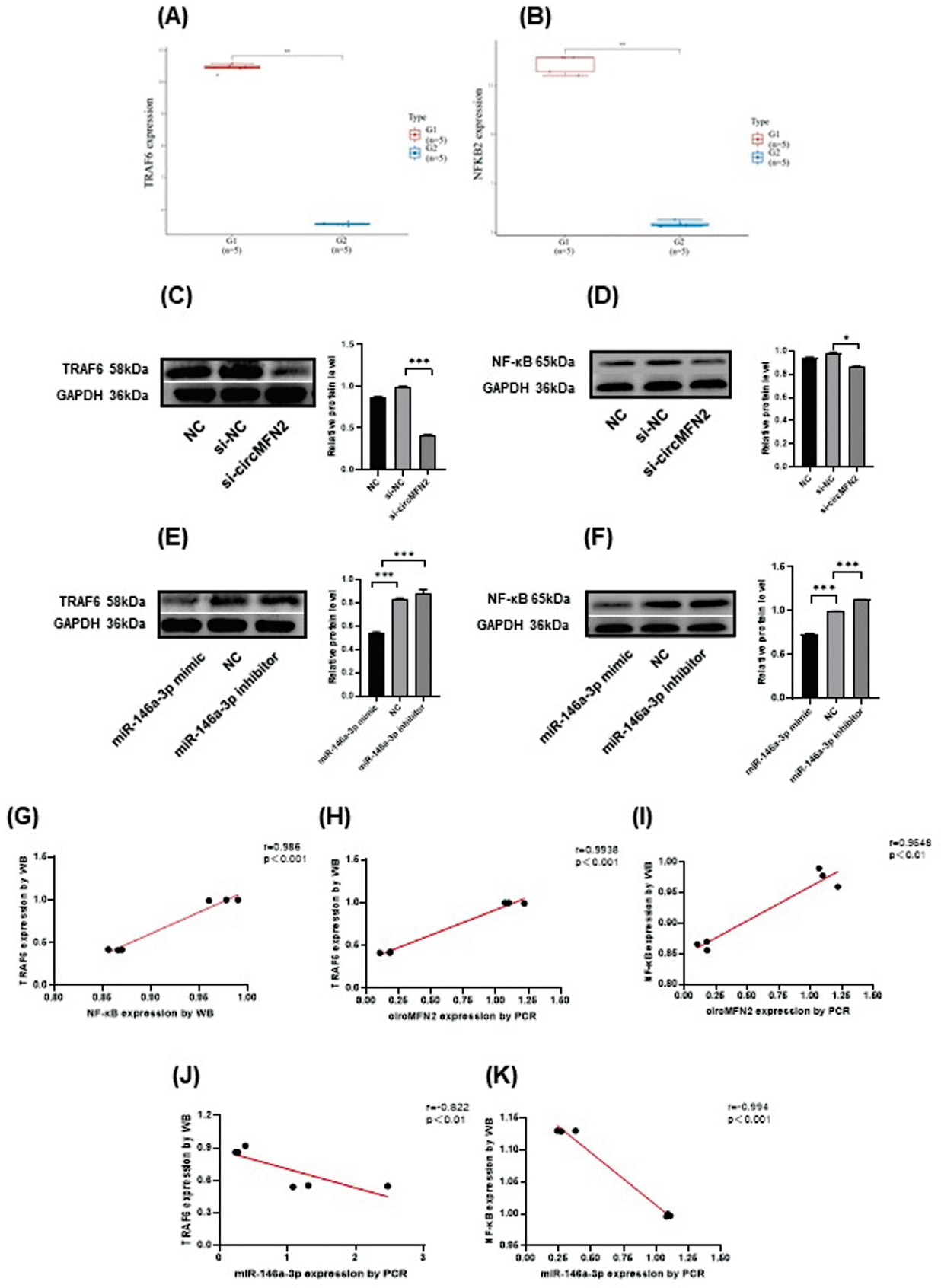

Fig. 7 circMFN2 regulate the PA cells tumorigenesis via miR-146a-3p-TRAF6/ NF-?B signal axis.

 © 2024. The Author(s).

Researchers have found that certain circRNAs present in the nucleus can influence their own transcriptional activity by binding to RNA polymerase II. Additionally, they can promote the expression of their parental genes by interacting with the U1 small ribonucleoprotein and the parental gene promoter, thereby enhancing the expression of these genes.[30,31] At the same time, the methylation modification of circRNA has also received widespread attention in the academic community. Modified circRNAs with m6A modification can recruit molecules such as YTHDF3, initiating the protein translation process. Moreover, circRNAs themselves can also engage in translational work. By identifying open reading frames (ORFs) within circRNAs, researchers have associated relevant ribosomal entry sites.[31] Analysis using the red fluorescent protein (RFP) dataset revealed that some circRNAs have specific RFP binding sites, indicating a significant connection between circRNAs and translated ribosomes.

However, little research has been done on the pattern of circRNA expression and its clinical importance in PA.[32] Especially for PA-related targets and gene prediction, there is no good database to provide data support. Our study revealed that circMFN2 exhibited significant upregulation in aggressive PAs and demonstrated a positive correlation with tumor growth, cellular transport, and cellular morphology. This was determined through the analysis of invasive and noninvasive adenoma samples by retrieving PA-related high-throughput microarrays using the gene expression omnibus (GEO) and KEGG methods. According to our findings, there appears to be a correlation between the expression of circMFN2 and the presence of invasion, as well as the need for surgery. Specifically, the invasive group had higher levels of circMFN2 expression compared with the noninvasive group. Based on testing of the clinical samples, including serum, exosome, and tissue. CircMFN2 expression was significantly lower before and after surgery in the same patients. The current experimental results demonstrate that removal of adenomas through surgery can lead to changes in the level of circMFN2 in the blood of patients. It is important to note that the majority of circRNA originates from the nucleus and is subsequently secreted into the cytoplasm. The resection of tumor cells in adenomas results in a reduction in the level of circMFN2, which plays a role in regulating cell growth and invasion. This reduction in adenoma cells consequently impacts the level of circMFN2 in the serum. Additionally, the altered levels of hormones secreted by pituitary tumors in humans after adenoma removal can affect the protein-mRNA-circRNA alterations, thereby influencing the levels of circMFN2. More importantly, the efficacy of circMFN2 for the possible diagnosis of PA was analyzed using ROC curves, and the results showed that circMFN2 has a promising ability to serve as an independent diagnostic indicator and molecular marker for the diagnosis of PA. These findings imply that the pathophysiology and development of PA may be influenced by the expression of circMFN2.

It is equally important to elaborate on the function of circMFN2 in PA cells. We explored its effects on tumorigenesis and motility by knocking down the target gene and completing in vitro experiments. Our results demonstrated that circMFN2 downregulation could effectively inhibit the biological function of PA cells, such as proliferation and migration. To further validate the circMFN2 mechanism in PA, we identified the miRNAs downstream of circMFN2 in several databases using bioinformatic analysis and qRT–PCR and found that miR-146a-3p may play a biological role as a molecular sponge of circMFN2 in PA cells. We performed transfection experiments using miR-146a-3p mimics and an miR-146a-3p inhibitor and rescue experiments using si-circMFN2 to verify the ability of circMFN2 to regulate proliferation and migration of PA cells through miR-146a-3p. The results show that miR-146a-3p acts as an antioncogene by inhibiting its proliferation and motility. It was also observed that circFMN2 and miR-146a-3p have a competitive binding at the 3′UTR site. When circFMN2 and miR-146a-3p were simultaneously knocked down, the effect on PA cells was successfully rescued. These findings suggested that circMFN2 may regulate the tumorigenic process of PAs through its interaction with miR-146a-3p.

Within the miRNA-mRNA regulatory network, we used bioinformatic techniques to identify downstream molecules linked to tumor growth and motility. The study found that an individual mRNA can bind with multiple miRNAs to produce regulatory effects. The TRAF6/NF-κB pathway was identified as the most suitable pathway for our theory which binds to miR-146a-3p. TARF6/NF-κB, which is present in almost all human cells and associated with p50 and p52, can be activated by various stimuli and plays a crucial role in regulating apoptosis, cell differentiation, and cellular inflammation. To verify this hypothesis, we detected changes in TRAF6 and NF-κB when circMFN2 and miR-146a-3p were upregulated or downregulated. The results showed that knocking down circMFN2 downregulated TRAF6/NF-κB expression. However, the miR-146a-3p knockdown results were opposite of the circMFN2 knockdown results. Thus, miR-146a-3p was negatively correlated with TRAF6/NF-κB. Several pieces of evidence have also suggested that TNF-α can induce the development and progression of epithelial–mesenchymal transition (EMT) via TRAF6/NF-κB.[33] Ma et al found that CCL3 promotes proliferation of colorectal cancer related with TRAF6/NF-κB molecular pathway,[34] and Deng et al found that the TRAF6/NF-κB pathway was associated with early brain injury after subarachnoid hemorrhage.[35] According to Vergani et al, miR-146a-5p impairs melanoma resistance to kinase inhibitors by targeting COX2 and regulating NF-κB-mediated inflammatory mediators.[36] Based on these studies, we made the following conclusion. CircMFN2 affects cell proliferation in PA cells by partially regulating the TRAF6/NF-κB axis through miR-146a. The cause of cell proliferation may be that TRAF6/NF-κB is a key player in regulating cell growth and gene transcription. When the signaling factor TNF binds to the cell membrane receptor, it triggers a series of events that activate TRAF6/NF-κB. The conformational change in the receptor allows it to transmit the signal to IKK kinase (IkB kinase), which then phosphorylates the IkB protein. This phosphorylation leads to the dissociation of IkB from the trimeric complex, freeing TRAF6/NF-κB to act, which allows it to rapidly move from the cytoplasm into the nucleus. In the nucleus, TRAF6/NF-κB binds to specific sequences on nuclear deoxyribonucleic acid

 © 2024. The Author(s).

(DNA), promoting the transcription of genes involved in cell growth and proliferation, such as CyclinD1, c-Myc, MMP-9, and VEGF.[37–40] It is important to note that sustained activation of this pathway can lead to uncontrolled cell growth. The reason for cell migration and invasion may be TRAF6/NF-κB. The change of TRAF6/NF-κB expression affects the expression of E-cadherin and N-cadherin protein, loosens the connection between cells, promotes the EMT process of cells, and then increases the migration and invasion ability of PA cells.[41]

To summarize, we investigated whether circMFN2 can be used as a molecular marker to distinguish PA patients from healthy individuals. Our study first provided evidence that the critical regulatory effects of circMFN2/miR-146a-3p/TRAF6/NF-kB pathway on pituitary adenoma tumorigenesis. Therefore, a novel discovered regulatory feedback loop constituted by circMFN2/miR-146a/TRAF6/NF-κB in PA was exposed by us. But based on the findings of this study, we still need to improve the animal experiments and multicenter collection of patient data for statistical analysis to produce more accurate results. At present, circRNA-RBP is still a research hotspot in the academic field, but there is no research on the downstream RNA-binding protein (RBP) of circMFN2, so we will further study its downstream RBP to clarify its detailed mechanism of action, and after clarifying the mechanism, we will be able to target the inhibition of circMFN2, and carry out a large-scale clinical trial to explore its potential for the treatment of PAs.

Conclusion

We identified that circMFN2, as a potential oncogene acting through miR-146a-3p in PA cells, may affect the pathogenesis of PA via the TRAF6/NF-κB axis. CircMFN2 has a specific reference value as a molecular marker for diagnosing PA serum, exosome, and tissue. By unearthing this remarkable association, we offered new ideas and targets for the diagnosis of PA.

Availability of Data and Materials

We guarantee the authenticity and validity of all data and results. Open up some of the raw data uploads as supplementary files.

Ethics Approval

All the patients' blood and tissue were collected after obtaining written signed informed consent and validated by the Ethics Committee of The First Affiliated Hospital of Medical College of Shihezi (KJ2021–076–02).

Informed Consent

Informed consent was obtained from all individuals included in this study.

Author Contributions

Q.L. contributed to project management and manuscript editing. H.W. completed the manuscript writing and data analysis and performed an experiment. X.G. was involved in clinical sample collection. Z.Y. assisted in the investigation. L.W. and Y.Q. designed the experiment. All the authors reviewed the article.

Funding

This study was supported by the XPCC Science and Technology Plan of Science and Technology Innovation Talent Program (2022CB002–09) to Qi Liu.

Conflict of Interest

None declared.

References

1 Melmed S. Pituitary-tumor endocrinopathies. N Engl J Med 2020; 382(10):937–950
2 Tatsi C, Stratakis CA. Aggressive pituitary tumors in the young and elderly. Rev Endocr Metab Disord 2020;21(02):213–223
3 Asa SL, Mete O, Perry A, Osamura RY. Overview of the 2022 WHO classification of pituitary tumors. Endocr Pathol 2022;33(01): 6–26
4 Mercer TR, Mattick JS. Structure and function of long noncoding RNAs in epigenetic regulation. Nat Struct Mol Biol 2013;20(03): 300–307
5 Cocquerelle C, Mascrez B, Hétuin D, Bailleul B. Mis-splicing yields circular RNA molecules. FASEB J 1993;7(01):155–160
6 Memczak S, Jens M, Elefsinioti A, et al. Circular RNAs are a large class of animal RNAs with regulatory potency. Nature 2013;495 (7441):333–338
7 Jeck WR, Sorrentino JA, Wang K, et al. Circular RNAs are abundant, conserved, and associated with ALU repeats. RNA 2013;19(02): 141–157
8 Salzman J, Gawad C, Wang PL, Lacayo N, Brown PO. Circular RNAs are the predominant transcript isoform from hundreds of human genes in diverse cell types. PLoS One 2012;7(02):e30733
9 Louro R, El-Jundi T, Nakaya HI, Reis EM, Verjovski-Almeida S. Conserved tissue expression signatures of intronic noncoding RNAs transcribed from human and mouse loci. Genomics 2008;92 (01):18–25
10 Lu J, Zhang PY, Li P, et al. Circular RNA hsa_circ_0001368 suppresses the progression of gastric cancer by regulating miR-6506-5p/FOXO3 axis. Biochem Biophys Res Commun 2019;512(01): 29–33
11 Ghosh S, Chan CK. Analysis of RNA-seq data using TopHat and cufflinks. Methods Mol Biol 2016;1374:339–361
12 Wang K, Singh D, Zeng Z, et al. MapSplice: accurate mapping of RNA-seq reads for splice junction discovery. Nucleic Acids Res 2010;38(18):e178
13 Ritchie ME, Phipson B, Wu D, et al. limma powers differential expression analyses for RNA-sequencing and microarray studies. Nucleic Acids Res 2015;43(07):e47
14 Wu T, Hu E, Xu S, et al. clusterProfiler 4.0: a universal enrichment tool for interpreting omics data. Innovation (Camb) 2021;2(03): 100141
15 He Q, Li Z, Yin J, et al. Prognostic significance of autophagy-relevant gene markers in colorectal cancer. Front Oncol 2021; 11:566539
16 Chatzellis E, Alexandraki KI, Androulakis II, Kaltsas G. Aggressive pituitary tumors. Neuroendocrinology 2015;101(02):87–104
17 Xu D, Wang L. The involvement of miRNAs in pituitary adenomas pathogenesis and the clinical implications. Eur Neurol 2022;85 (03):171–176
18 Beylerli O, Beeraka NM, Gareev I, et al. MiRNAs as noninvasive biomarkers and therapeutic agents of pituitary adenomas. Int J Mol Sci 2020;21(19):7287

 © 2024. The Author(s).

19 Inoshita N, Nishioka H. The 2017 WHO classification of pituitary adenoma: overview and comments. Brain Tumor Pathol 2018;35 (02):51–56
20 Vo JN, Cieslik M, Zhang Y, et al. The landscape of circular RNA in cancer. Cell 2019;176(04):869–881.e13
21 Chen L, Wang C, Sun H, et al. The bioinformatics toolbox for circRNA discovery and analysis. Brief Bioinform 2021;22(02): 1706–1728
22 Zhang HD, Jiang LH, Sun DW, Hou JC, Ji ZL. CircRNA: a novel type of biomarker for cancer. Breast Cancer 2018;25(01):1–7
23 Yan H, Bu P. Non-coding RNA in cancer. Essays Biochem 2021;65 (04):625–639
24 Ma C, Wang X, Yang F, et al. Circular RNA hsa_circ_0004872 inhibits gastric cancer progression via the miR-224/Smad4/ ADAR1 successive regulatory circuit. Mol Cancer 2020;19(01): 157
25 Liu J, Li J, Su Y, Ma Z, Yu S, He Y. Circ_0009910 serves as miR-361-3p sponge to promote the proliferation, metastasis, and glycolysis of gastric cancer via regulating SNRPA. Biochem Genet 2022;60 (05):1809–1824
26 Wang D, Ming X, Xu J, Xiao Y. Circ_0009910 shuttled by exosomes regulates proliferation, cell cycle and apoptosis of acute myeloid leukemia cells by regulating miR-5195-3p/GRB10 axis. Hematol Oncol 2021;39(03):390–400
27 Deng N, Li L, Gao J, et al. Hsa_circ_0009910 promotes carcinogenesis by promoting the expression of miR-449a target IL6R in osteosarcoma. Biochem Biophys Res Commun 2018;495(01): 189–196
28 Li X, Li C, Zhang L, et al. The significance of exosomes in the development and treatment of hepatocellular carcinoma. Mol Cancer 2020;19(01):1
29 Kim H, Wang SY, Kwak G, Yang Y, Kwon IC, Kim SH. Exosome-guided phenotypic switch of M1 to M2 macrophages for cutaneous wound healing. Adv Sci (Weinh) 2019;6(20):1900513
30 Chen X, Mao R, Su W, et al. Circular RNA *circHIPK3* modulates autophagy via *MIR124-3p*-STAT3-PRKAA/AMPKα signaling in STK11 mutant lung cancer. Autophagy 2020;16(04):659–671
31 Du WW, Yang W, Xuan J, et al. Reciprocal regulation of miRNAs and piRNAs in embryonic development. Cell Death Differ 2016;23 (09):1458–1470
32 Zhang W, Chen S, Du Q, et al. CircVPS13C promotes pituitary adenoma growth by decreasing the stability of IFITM1 mRNA via interacting with RRBP1. Oncogene 2022;41(11):1550–1562
33 Zinatizadeh MR, Schock B, Chalbatani GM, Zarandi PK, Jalali SA, Miri SR. The nuclear factor kappa B (NF-kB) signaling in cancer development and immune diseases. Genes Dis 2020;8(03): 287–297
34 Ma X, Su J, Zhao S, et al. CCL3 promotes proliferation of colorectal cancer related with TRAF6/NF-κB molecular pathway. Contrast Media Mol Imaging 2022;2022:2387192
35 Deng HJ, Deji Q, Zhaba W, et al. A20 establishes negative feedback with TRAF6/NF-κB and attenuates early brain injury after experimental subarachnoid hemorrhage. Front Immunol 2021; 12:623256
36 Vergani E, Dugo M, Cossa M, et al. miR-146a-5p impairs melanoma resistance to kinase inhibitors by targeting COX2 and regulating NFkB-mediated inflammatory mediators. Cell Commun Signal 2020;18(01):156
37 Hu YL, Feng Y, Chen YY, et al. SNHG16/miR-605-3p/TRAF6/NF-κB feedback loop regulates hepatocellular carcinoma metastasis. J Cell Mol Med 2020;24(13):7637–7651
38 Tian H, Liu Z, Pu Y, Bao Y. Immunomodulatory effects exerted by *Poria cocos* polysaccharides via TLR4/TRAF6/NF-κB signaling in vitro and in vivo. Biomed Pharmacother 2019;112:108709
39 Gao W, Zhang Y. Depression of lncRNA MINCR antagonizes LPS-evoked acute injury and inflammatory response via miR-146b-5p and the TRAF6-NFkB signaling. Mol Med 2021;27(01):124
40 Lv F, Huang Y, Lv W, et al. MicroRNA-146a ameliorates inflammation via TRAF6/NF-κB pathway in intervertebral disc cells. Med Sci Monit 2017;23:659–664
41 Lin K, Baritaki S, Militello L, Malaponte G, Bevelacqua Y, Bonavida B. The role of B-RAF mutations in melanoma and the induction of EMT via dysregulation of the NF-κB/snail/RKIP/PTEN circuit. Genes Cancer 2010;1(05):409–420

 © 2024. The Author(s).